Miniaturization of Conical Helical Antenna via Optimized Coiling

Tao Peng [1], Stavros Koulouridis [2], and John L. Volakis[1]

[1] ElectroScience Laboratory, Department of Electrical and Computer Engineering
The Ohio State University, Columbus, OH, 43212, U.S.A.
peng.75@osu.edu, volakis.1@osu.edu

[2] Laboratory of Electrotechnics, Department of Electrical & Computer Engineering
University of Patras, Patras, 26500, Greece
koulouridis@ece.upatras.gr

Abstract **─** Conical helices are extensively used in multifunctional antenna platforms for UHF and VHF frequencies because of their broadband characteristics. Therefore, there is strong interest to reduce their size as much as possible. In this paper, a conical helix with metallic ground plane is considered and reduced in size by as much as 30% via coiling (equivalent to inductive loading). The coiling is obtained via genetic algorithms subject to customized criteria for best ultra-wideband realized gain.

Index Terms **─** Antenna optimization, circular polarized antennas, equivalent circuit model, Genetic Algorithm, UWB antenna miniaturization.

I. INTRODUCTION

The benefits of ultra wideband antennas have been increasingly attractive due to their intrinsic capability to integrate multiple communication systems on a single platform. Axial mode conical helix is one of the widely used ultra wideband (UWB) circular polarized antennas for satellite communications. To integrate such an antenna for airborne, ground and sea based systems, its size and weight must be minimized. Otherwise, it can be prohibitively large for low frequency applications and too heavy for airborne systems. In this paper, inductive loadings are used to reduce the antenna aperture size as much as possible with minimal negative impact on the wideband gain. For our applications, it is desired to have total realized gain over -15 dBi at the lowest frequencies, and realized right hand circular polarized (RHCP) gain as high as possible for the ultra-wideband section.

Conical helices backed by a metallic surface are characterized by good directive circular polarized (CP) gain and over 50% bandwidth [1]. We build on the extensive background relating to the axial modes of these antennas [1-[6], with a goal to reduce their size. Specifically, we introduce inductive loading in the form of coiling to slow down wave velocity [7-9] along the helical antenna wires. We note that adding coiling increases the wire length forming the conical helix, leading to miniaturization. However, if not done optimally, antenna gain at higher frequencies would be reduced.

An important aspect of our study is the optimization methodology for the coiling. Coiling can certainly add miniaturization but if it is not optimally applied, it reduces gain and bandwidth. Here, genetic algorithm (GA) optimization [10] is employed to minimize bandwidth degradation. Indeed, GA optimization was applied to different helical antennas using moment method analysis with curved segments in [11]. In this paper, a moment method wire code was also used, namely NEC-Win [12], to carry out the optimization.

Below, we discuss the key geometric parameters of the coiled conical helix and the proposed miniaturization concept. A carefully constructed GA fitness function to generate highly customized wideband CP gain is adopted. Optimization results show a 30% to 40% size reduction, subject to the constraint set. We should note here that all simulations are carried out with copper wires to take into consideration the resistive loss. One might think that long wiring from coiling would degrade antenna efficiency. However, ohmic loss attributes significantly to the impedance matching at lower frequencies where the small antenna tends to behave more like a resonator. In this case, ohmic loss may benefit antenna realized gain at these low frequencies because better matching from resistive loss can balance or even outweigh the gain loss.

II. ANTENNA GEOMETRY AND PARAMETRIC CHARACTERIZATION

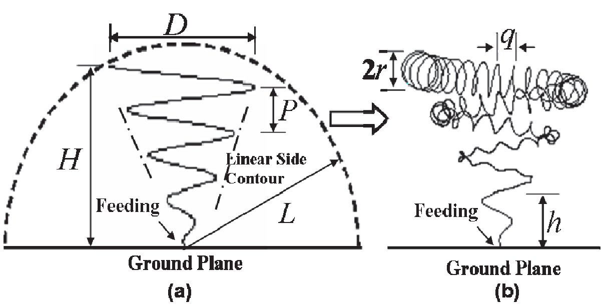

Fig. 1. (a) Geometric parameters of a conical helix antenna. The enclosing sphere of radius L defines the size restrictions for the antenna; (b) details of the coiling.

Our goal, as said, is to minimize antenna size. To do so we need to determine all the optimization parameters that we will deal with. In Fig. 1a, the geometric parameters of the conical helix are given, that is the height H, the step P and helix top diameter D. Additionally, a side contour line (Fig. 1a) determines how the helix diameter changes with the height from the feeding to the end tip of the helical wire (in Fig. 1a side contour line is linear). As for the coiling (see Fig. 1b) parameter h determines at what point from the ground the coiling starts. r and q determine the coil radius and pitch respectively. As it will be explained below, r and q variation along the helical wire is governed by a mathematical relation.

The size of an electrical small antenna is defined by its radian sphere [13], which is a hypothetical sphere whose diameter $2L$ is equal to the largest linear dimension of the antenna that it encloses (see Fig. 1a). We will keep our design restricted in such a sphere. That is, increasing top helix diameter will decrease helix's height and vice versa. The top diameter of the conical helix is limited by the radian sphere: $D = 2\sqrt{L^2 - H^2}$. Larger D leads to higher realized CP gain at lower frequencies in the $\theta = 0°$ direction. However, due to the radian sphere limitations, larger diameter D is translated to reduced antenna height H, and thus, the conical helix is more likely to be shorted by the mirror effects of the ground plane. Given this set of tradeoff, the optimal H is left for the optimizer to decide.

Another degree of freedom is the side conical contour line of the conical helix. In Fig. 1, the diameter of the conical helix increases linearly with the antenna height, so the side contour is linear. We can expand the potential antenna configurations by varying the side line of the conical helix (see Fig. 2a). In Fig. 2b, various contour lines are presented. They are divided in concave (upper left half of Fig. 2b) and convex curves (down right half of Fig. 2b). Parameters $\alpha_{1,contour}$ and $\alpha_{2,contour}$ (see Fig. 2) determine the type of concave and convex curve respectively as represented from the following line equations:

$$x^1 = R\left(1-\alpha_{1,contour}\arctan\left(\left(1-\frac{z}{H}\right)\tan\frac{1}{\alpha_{1,contour}}\right)\right), \quad (1)$$

$$x^2 = R\left(1-\tan\left(\left(1-\frac{z}{H}\right)\frac{1}{\alpha_{2,contour}}\right)/\tan\left(\frac{1}{\alpha_{2,contour}}\right)\right), \quad (2)$$

where x^1 or x^2 determines the helix radius at height z. Also R is the top helix radius ($R=D/2$).

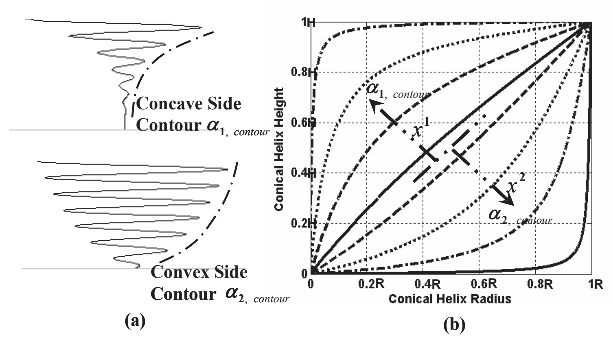

Fig. 2. The variation of helix radius x with increasing height z is defined by its contour line. The contours in the upper left half (concave curves) are determined by $\alpha_{1,contour}$ (eq. (1)); $\alpha_{2,contour}$ (eq. (2)) determines the contours in the down right half (convex curves).

Inductive loading to further slow down wave velocity is the key element for the conical helix miniaturization. Additional inductance will be introduced to the helical antenna by coiling its wire. Actually, under certain conditions, the coiling of the coiled conical helical antenna (coil radius r and coil pitch q, see Fig. 4a), can be considered as a helical waveguide. Under a dense helical coil condition $(2r >> q)$, its characteristic coil axial phase velocity is approximated by Rowe in [14]:

$$v_0 = \frac{1}{\sqrt{L_e C_e}} \approx \frac{cq}{2\pi r}\sqrt{\frac{I_0(\gamma r)K_0(\gamma r)}{I_1(\gamma r)K_1(\gamma r)}}, \quad (3)$$

where γ is the spatial frequency in the coil radial direction, and c is the speed of light. $I_{0,1}$ and $K_{0,1}$ are the zeroth/first order modified Bessel functions of the first and second kind respectively. The dispersion equation of the helical coil waveguide transmission line can be obtained as

$$\gamma^2 = k^2\left(\frac{2\pi r}{q}\right)^2 \frac{I_1(\gamma r)K_1(\gamma r)}{I_0(\gamma r)K_0(\gamma r)}, \quad (4)$$

with $k^2 = \omega^2 \mu\varepsilon$. Clearly, the larger the r and the smaller the q, the slower the axial phase velocity v_0 [14] is. As the wave is slowed down more, miniaturization is achieved.

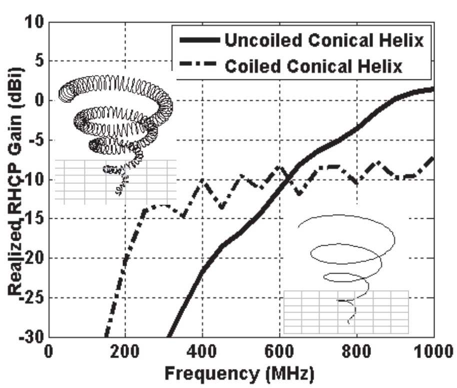

Fig. 3. Coiling should be carried out in an optimum way; otherwise it could severely damage the wideband gain of the conical helix antenna.

The main side effect of lager r and smaller q throughout conical helical wires is the severe gain degradation at higher frequency regions as shown in Fig. 3. This is partly due to the strong resonance caused by large equivalent transmission line inductance L_e and capacitance C_e of the helical coil waveguide. We refer to Rowe [14] here as well:

$$L_e = \frac{2\pi\mu_0 r^2}{q^2} I_1(\gamma r)K_1(\gamma r), \quad (5)$$

$$C_e = \frac{2\pi\varepsilon_0}{I_0(\gamma r)K_0(\gamma r)}. \quad (6)$$

Both L_e and C_e increase almost linearly with the ratio r/q as shown in Fig. 4b and 4c. Excessively large L_e and C_e from high r/q (large r, small q) transforms the conical helix antenna from a radiator into a transmission line at the UWB frequency range, which makes good impedance matching impossible and reduces the realized CP gain significantly. Hence, the proper design of the coiling is the most crucial part in miniaturizing a conical helix antenna as much as possible without reducing the wideband CP gain or degrading the bandwidth.

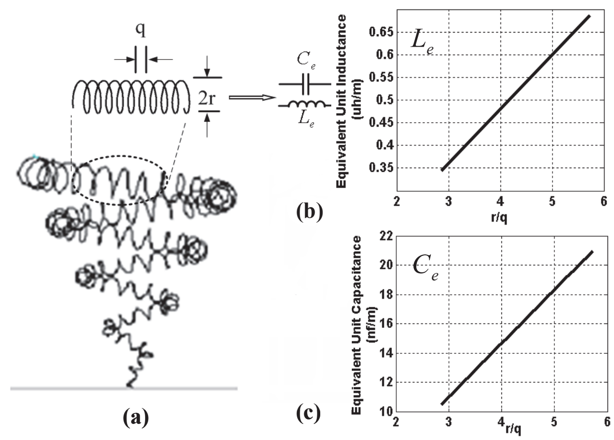

Fig. 4. The equivalent inductance and capacitance of the coiling increase almost linearly with the r/q ratio. Excessively large r and small q can change the conical helix antenna from a radiator to a resonator with large values of equivalent inductance L_e and capacitance C_e (eqs. (5) and (6)).

To keep impedance matching of the loaded coil waveguide well maintained, it is important to slowly increase inductance using, for example, a gradually increasing coil diameter of maximum value $2r$, and a gradually decreasing coil pitch from q_1 at the bottom to q_2 at top. Therefore, we will let the coil starting height h, the maximum coil radius at the top r, the coil pitch at the lower starting position q_1 and at the top q_2 to be optimized (see Fig. 1b). It is also important to note that the performance of the coiled conical helix is significantly influenced by how the coil radius changes from 0 to r and how the coil pitch varies from q_1 to q_2. Here again, we use the same tapering coefficient formula as the conical helix side contour lines in (1), (2) to characterize the growth of coil radius and the decrease of coil pitch. Note that $t(z)$ is the length of the helical wires from the source at height z and $T = t(H)$ is the total length of the conical helix wire.

$$r^1 = r\left(1 - \alpha_r^1 \arctan\left(\left(1 - \frac{t(z)}{T}\right)\tan\frac{1}{\alpha_r^1}\right)\right),$$

$$r^2 = r\left(1 - \tan\left(\left(1 - \frac{t(z)}{T}\right)\frac{1}{\alpha_r^2}\right)/\tan\left(\frac{1}{\alpha_r^2}\right)\right),$$

$$q^1 = q_1 + (q_2 - q_1)\left(1 - \alpha_q^1 \arctan\left(\frac{T - t(z)}{T - t(h)}\tan\frac{1}{\alpha_q^1}\right)\right),$$

$$q^2 = q_1 + (q_2 - q_1)\left(1 - \tan\left(\frac{T - t(z)}{T - t(h)}\frac{1}{\alpha_q^2}\right)/\tan\left(\frac{1}{\alpha_q^2}\right)\right).$$

Again, α_r^1 or α_r^2 and α_q^1 or α_q^2 correspond to concave (α_r^1, α_q^1) or convex (α_r^2, α_q^2) curves and they allow for considerable coil radius and pitch variations. The coiling along the helical wires at location $t(z)$ has a radius r^1 or r^2, and a pitch q^1 or q^2.

In conclusion, by utilizing various geometric parameters for the helical antenna, we increase our chances of finding the best miniaturized coiled conical helix within the specific radian sphere limitation. The geometrical parameters to optimize are the height H and step P of conical helix, and the side contour line parameter $\alpha_{1,contour}$ or $\alpha_{2,contour}$. Several inductive coiling structures are then modeled by optimizing maximum coil radius at the top r, lower coil pitch q_1, top coil pitch q_2, coil starting height h, coil radius tapering parameter α_r^1 or α_r^2, and coil pitch tapering parameter α_q^1 or α_q^2. These nine optimization variables allow abundant different geometrical configurations of the coiled conical helix with enough flexibility to get optimum antenna directivity, axial ratio and radiation patterns. Further, since impedance matching or VSWR is also very important, especially at lower resonating frequencies, we add the line characteristic impedance as the tenth optimization variable for optimal antenna matching.

III. OBJECTIVE FUNCTION

For optimization, it is critical to choose an accurate problem-descriptive objective function. Such a function should seek the smallest antenna with the largest possible bandwidth and gain. In our design, we are mostly concerned for the -15dBi and 0 dBi gain points, as well as wideband axial ratio. With this in mind, we choose to maximize the following objective function,

$$F_{obj}(r,h,q) = \sum_{i=1}^{M} \min\left\{ \left[\max(G_i, G_i^{lower}) - G_i^{upper}\right]^3 + \left[\max\ (G_i, G_i^{lower}) - G_i^{upper}\right],\ 0 \right\} \cdot w_i + \sum_{j=1}^{N} \max\left\{ \left[\min(AR_j, AR_j^{upper}) - AR_i^{lower}\right]^3 + \left[\min(AR_j, AR_j^{upper}) - AR_j^{lower}\right],\ 0\right\} \cdot w_j^{AR}$$

The objective function comprises two sum terms and seeks to concurrently increase realized CP gain and decrease axial ratio in the $i = 1,2,3 \cdots M$ and j = $1,2,3 \cdots N$ frequency regions respectively. w_i and w_j are constants (weights) that are used to regulate the contribution of the different terms.

In the first sum term (CP gain), G_i (to be maximized) is the mean value of 3 frequency samples in the i th region and is evaluated against a pre-specified lower bound G_i^{lower}. The maximum of the two, viz. $\max(G_i, G_i^{low})$, is then contrasted with an upper pre-specified bound G_i^{upper}. The idea is to favor values of gain that lie in the $(G_i^{lower}, G_i^{upper})$ area. Values that are below G_i^{lower} are penalized with the maximum negative penalty, equal to

$$(G_i^{lower} - G_i^{upper})^3 + (G_i^{lower} - G_i^{upper}).$$

Values of G_i in the $(G_i^{lower}, G_i^{upper})$ area result to a varying negative value of

$$\left(G_i - G_i^{upper}\right)^3 + \left(G_i - G_i^{upper}\right).$$

Values over G_i^{upper} are not penalized but do not get either any benefit since they result to a value equal to zero. In that way, very low values of G_i do not de-normalize the objective function. Also, very high values of G_i are unwanted since they can destroy the gain behavior at other frequency regions.

The cubic term $\left[\max\left(G_i, G_i^{low}\right) - G_i^{upper}\right]^3$ and the linear term $\left[\max\left(G_i, G_i^{low}\right) - G_i^{upper}\right]$ are employed to obtain a descriptive measure of the gain performance for the different frequency bands, that is gain differences smaller than unity are mainly controlled from the linear term, whereas gain differences larger than unity are emphasized through the cubic term.

Axial ratio minimization which is controlled from the second sum term of the objective function is carried out through a similar scheme.

IV. RESULTS AND DISCUSSION

The optimizing antenna was enclosed in a sphere with $L = 4.5''$ radius (see Fig. 1). As said, GA optimization was adopted. Details on the GA can be found in [10], [15]. As noted, the height H, pitch P, and the side contour curvature parameter $\alpha_{contour}$ (see Fig. 2) completely describe the shape of the conical helix. The top helix radius is determined from $R = D/2 = \sqrt{L^2 - H^2}$. In genetic algorithm, the height H ranged from $0.8''$ to $4.3''$ with 16 possible values in between. The pitch P was set as $H/8 \le P \le H$ with 8 possible values. The side contour parameter of the conical helix ranged $0.64 \le \alpha_{contour} \le 1.44$ with 64 potential curves. There was one extra digit to define whether $\alpha_{1,contour}$ or $\alpha_{2,contour}$ is adopted ($\alpha_{1,contour}$ shows concave curves and $\alpha_{2,contour}$ represents convex curves in Fig. 2b). The coiling configuration was determined by maximum radius r, starting and ending pitches q_1, q_2, the coiling starting height, h, and two tapering parameters α_r and α_q that describe how the coil radius and coil pitch grow from 0 to r and from q_1 to q_2. α_r and α_q were set as $\alpha_{contour}$: $0.64 \le \alpha_r, \alpha_q \le 1.44$ with 64 values and two extra digits to distinguish between α_r^1, α_q^1 and α_r^2, α_q^2 respectively. These two parameters are very crucial to characterize how fast the coil radius grows and coil pitch decreases. For optimization, we specifically allowed r to vary over $0'' < r < 0.8''$ with 8 potential values and $0.1'' < q_2 \le q_1 < 5''$ with 64 potential values for each. Also, the coiling starting height variation range was set to $0'' \le h \le 0.8 \times H$ and was allowed to take 8 different values. The matching impedance varied from 50Ω to 500Ω with 8 possible values to achieve the optimal matching loss. The resulting GA chromosome had 49 bits length. 50 "individuals" were sufficient to cover the design space. In addition, 70% crossover and 2% mutation rates were employed with elitism and niching adapted within the GA. We note that convergence was typically achieved after 40 to 50 generations.

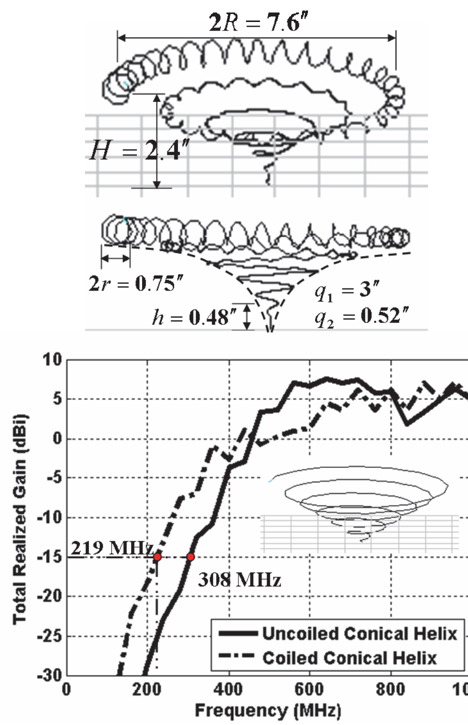

Fig. 5. Optimal coiled conical helix configuration within the $L = 4.5''$ radian sphere. It achieves around 30% miniaturization for the -15 dBi total gain point. ($\alpha_{1,contour} = 1.44$, $\alpha_r^2 = 0.69$, $\alpha_q^2 = 0.82$, $Z = 150\Omega$). The rest of the geometric parameters are given in the figure.

For this work, our goal was to achieve high wideband CP gain with the -15 dBi point as low as possible without affecting the 0 dBi corresponding frequency. To facilitate this, we also chose an intermediate frequency control point with a target gain of -5dBi. So for the objective function, after an examination of Fig. 3, we chose 230-270MHz, 430-470MHz and 950-990MHz as our 3 frequency bands ($i = 1, 2, 3$). For 230-270MHz (the -15dBi point region), G_1 is calculated from

$$G_1 = \frac{G_{f=230MHz} + G_{f=250MHz} + G_{f=270MHz}}{3},$$

with the corresponding G_i^{lower}, G_i^{upper} values chosen as $G_1^{lower} = -20$ and $G_1^{upper} = -13$. Likewise, for the 430-470MHz band, the gain G_2 is calculated from

$$G_2 = \frac{G_{f=430MHz} + G_{f=450MHz} + G_{f=470MHz}}{3},$$

with $G_2^{lower} = -10$ and $G_2^{upper} = 0$. Finally, for the higher frequency band (the 0dBi gain region), we chose

$$G_3 = \frac{G_{f=950MHz} + G_{f=970MHz} + G_{f=990MHz}}{3},$$

with $G_3^{lower} = -3$ and $G_3^{upper} = 3$. For the axial ratio optimization (second term of the objective function), we chose one band at 950-990MHz. We set

$$AF_1 = \frac{AR_{f=950MHz} + AR_{f=970MHz} + AR_{f=990MHz}}{3}$$

and we chose $AR_1^{upper} = 10$ and $AR_1^{lower} = 1.5$. As also noted in the fitness function, each of the gain "penalty" values is multiplied by a weighting term. For this optimization, since high broadband RHCP gain was of major interest, we set the weight $w_1 = w_2 = 1.2$, $w_3 = 1.5$ and $w_1^{AR} = 1.2$

In Fig. 5, we show the final optimized case and the corresponding realized gain. The optimized coiled helix has its -15 dBi total gain point miniaturized from 308MHz down to 219 MHz implying 30% miniaturization. As seen in Fig. 6, in both UHF and VHF bands, the coiled conical helix has better gain characteristics than the simple conical helix. Also, the axial ratios of the two antennas show comparable performance. It is notable, as shown in Fig. 7, that in the higher frequency region, the main lobe of the coiled conical helix at $\theta = 0°$ direction is more stable, and thus generates higher directivity. In contrast, the radiation pattern of the simple conical helix deteriorates in higher frequencies and tilts away from the $\theta = 0°$ direction.

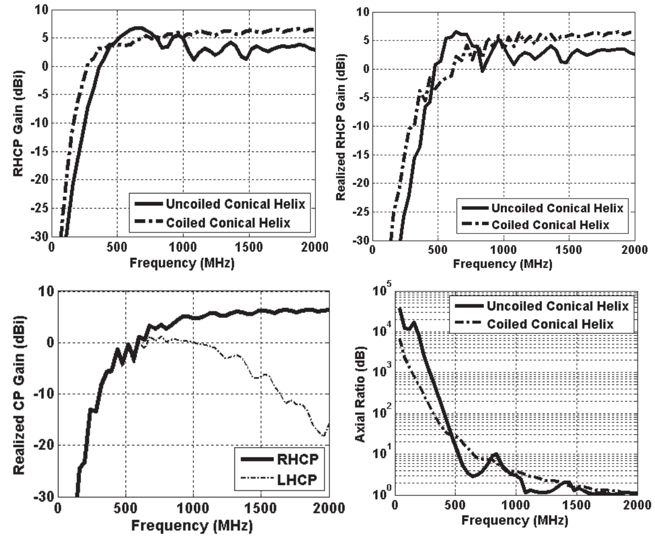

Fig. 6. The directivity and realized RHCP gains of the coiled conical helix are compared with those of the simple conical helix antenna over a broad bandwidth. Optimized coiled conical helix shows more miniaturization, higher wideband gain and comparable axial ratio.

In closing, we note that fabrication of the coiled conical helix is complex. As in [9], it can be realized using customized Beryllium copper coils. Coils with a tapered diameter and varying pitch can be manufactured by spring companies capable of making customized coils. Upright vertical boards can be employed to support the helix into specific concave contours to form the basic conical helix.

V. CONCLUSIONS

In this paper, we considered the minimization of a conical helix without appreciably compromising its broadband performance. To do so, we worked towards coiling the wire along the helical geometry. This should create an equivalent inductive loading and thus reduce the wave velocity along the spiral. The main challenge was to achieve best miniaturization without reducing high frequency gain. Hence, genetic algorithm (GA) optimization was adopted. A descriptive objective function was devised which weighted the performance variably at 3 different frequency bands, a low, an intermediate and a high frequency regions. This was found necessary as it is allowed to control the UWB antenna performance effectively. After establishing the optimization variables and fitness function, we proceeded to demonstrate a customized design example. As shown, simple coiling achieved a 30% size reduction without severe gain degradation in the higher wide band regions.

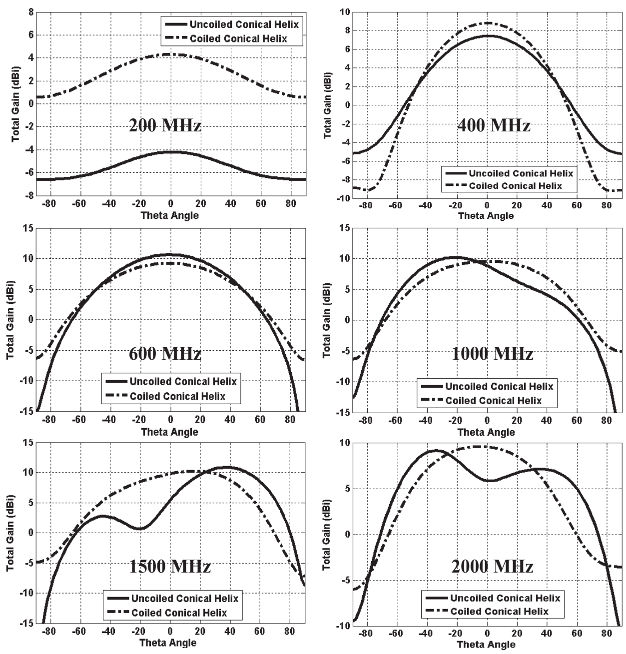

Fig. 7. Radiation patterns in the elevation plane of coiled conical helix and simple conical helix for different frequencies. At higher frequencies, coiled conical helix has more stable pattern and thus higher directivity than the simple conical helix.

REFERENCES

[1] H. E. King, J. L. Wong, and E. H. Newman, "Helical Antennas," ch. 12 in *Antenna Engineering Handbook* ed. by J. L. Volakis, McGraw-Hill, New York, 2007.

[2] J. D. Kraus and R. D. Marhefka, *Antennas*, 3rd ed., McGraw-Hill, New York, 2002.

[3] J. S. Chatterjee, "Radiation Field of a Conical Helix," *J. App. Physics*, vol. 24, no. 5, pp. 550-559, May 1953.

[4] V. H. Rumsey, "Frequency Independent Antennas," *IRE Int. Convention Record* vol. 5, pt. 1, pp. 114-118, Mar. 1957.

[5] J. D. Dyson and P. E. Mayes, "New Circularly-Polarized Frequency-Independent Antennas with Conical Beam or Omnidirectional Patterns," *IRE T. Antenna Propag.,* vol. 9, no. 4, pp. 334-342, Jul. 1961.

[6] J. L. Volakis, ed., *Antenna Engineering Handbook*, McGraw-Hill, New York, 2007.

[7] M. Lee, B. A. Kramer, C. C. Chen, and J. L. Volakis, "Distributed Lumped Loads and Lossy Transmission Line Model for Wideband Spiral Antenna Miniaturization and Characterization," *IEEE Trans. Antenna Propag.*, vol. 55, no. 10, pp. 2671-2678, Oct. 2007.

[8] B. A. Kramer, C. C. Chen, and J. L. Volakis, "Size Reduction of a Low-Profile Spiral Antenna Using Inductive and Dielectric Loading," *IEEE. Antenna Wirel. Pr.*, vol. 7, pp. 22-25, 2008.

[9] B. A. Kramer, "Size Reduction of an UWB Low-Profile Spiral Antenna," *Ph.D. Dissertation*, Ohio State University, 2007.

[10] Y. Rahmat-Samii and E. Michielssen, *Electromagnetic Optimization by Genetic Algorithms*, Wiley-Interscience, 1999.

[11] M. A. Mangoud, "Design of Circular Polarized Antennas using Genetic Algorithm based on Curved Wire Analysis," *Appl. Comput. Electrom.*, vol. 19, no. 3, pp. 177-183, Dec. 2004.

[12] G. J. Burke and A. J. Poggio, "Numerical Electromagnetic Code (NEC)--Method of Moments", Naval Ocean Systems Center, San Diego, Tech. Doc. NOSC TD 116, 1980.

[13] H. A. Wheeler, "The Radian Sphere around a Small Antenna," *Proceedings of the I.R.E.,* vol. 35, Aug. 1959.

[14] J. E. Rowe, *Nonlinear Electron-Wave Interaction Phenomena*, Academic Press, 1965.

[15] D. L. Carroll, FORTRAN Genetic Algorithm Driver, ver. 1.7, 1999. [Online]. Available: http://cuaerospace.com/carroll/ga.html